*J. Fluid Mech.* (2002), *vol.* 463, *pp.* 345–360.  
DOI: 10.1017/S0022112002008881 Printed in the United Kingdom

# Analysis of singular inertial modes in a spherical shell: the slender toroidal shell model

By M. RIEUTORD[1,2], L. VALDETTARO[4] AND B. GEORGEOT[3]

[1]Observatoire Midi-Pyrénées, 14 av. E. Belin, F-31400 Toulouse, France

[2]Institut Universitaire de France

[3]Laboratoire de Physique Quantique IRSAMC, Université Paul Sabatier, 118, Route de Narbonne F-31062 Toulouse Cedex 4, France

[4]Dipartimento di Matematica, Politecnico di Milano, Piazza L. da Vinci, 32, 20133 Milano, Italy

(Received 23 April 2001 and in revised form 1 March 2002)

We derive the asymptotic spectrum (as the Ekman number $E \to 0$) of axisymmetric inertial modes when the problem is restricted to two dimensions. We show that the damping rate of such modes scales with the square root of the Ekman number and that the width of the shear layers of the eigenfunctions scales with $E^{1/4}$. The eigenfunctions obey a Schrödinger equation with a quadratic potential; we provide the analytical expression for eigenvalues (frequency and damping rate). These results validate the picture that attractors act like a potential well, trapping inertial waves which resist confinement owing to viscosity. Using three-dimensional numerical solutions, we show that the results can be applied to equatorially trapped modes in a thin spherical shell; in fact, these two-dimensional solutions give the first step (the zeroth order) of a perturbative approach to three-dimensional solutions in a spherical shell. Our method is applicable in a straightforward way to any other container where bi-dimensionality dominates.

## 1. Introduction

Recently, Rieutord & Valdettaro (1997) and Rieutord, Georgeot & Valdettaro (2000, 2001) have shown, through the example of an incompressible fluid contained in a spherical shell, the fascinating behaviour of the oscillations of rotating fluids, namely inertial modes, which comes from the ill-posed nature of the associated inviscid problem.

Pressure perturbations of inviscid incompressible rotating fluids obey to the celebrated Poincaré equation, $\Delta p - (2\Omega/\omega)^2 \partial^2 p/\partial z^2 = 0$ where $\Omega$ is the angular velocity of the fluid's frame, $\omega$ the frequency of oscillations and $z$ the coordinate along the rotation axis. This equation is hyperbolic since $\omega \leqslant 2\Omega$ (Greenspan 1969). But for contained fluids pressure perturbations must meet boundary conditions expressing the impermeability of the boundaries; hence, the problem is mathematically ill-posed.

This property implies that, except for some containers (a full sphere, a cylinder) where the Poincaré equation is separable, most of the solutions of this problem are singular. As shown by Rieutord *et al.* (2001), three types of singularities arise. The first and strongest is the one associated with the convergence of the characteristics towards a periodic orbit called an attractor (Maas & Lam 1995; Rieutord & Valdettaro 1997).

Such singularities make the velocity field neither integrable nor square-integrable; equivalently, both total momentum and total kinetic energy of the fluid diverge. The second type of singularity comes about because of the oblique nature of boundary conditions: the impermeability of boundaries makes the velocity tangential to the boundaries, a condition which reads

$$-(\omega/2\Omega)^2 \boldsymbol{n}\cdot\nabla p + \mathrm{i}(\omega/2\Omega)(\boldsymbol{e}_z\times\boldsymbol{n})\cdot\nabla p + (\boldsymbol{e}_z\cdot\boldsymbol{n})(\boldsymbol{e}_z\cdot\nabla p) = 0$$

when using the pressure (Greenspan 1969) ($\boldsymbol{n}$ and $\boldsymbol{e}_z$ are unit vectors along the outer normal and $z$-axis respectively). A singularity arises when the boundary is parallel to a characteristic, a situation occurring at the so-called critical latitudes in a spherical shell (these latitudes $\lambda_c$ are such that $\sin\lambda_c = \omega/2\Omega$). These singularities leave the velocity field integrable but still forbid square-integrability. Finally, in the case of axisymmetric containers, an additional singularity of solutions focused on attractors comes into play (see the Appendix of Rieutord & Valdettaro 1997). It occurs on the symmetry axis but unlike the previous two singularities this one leaves the solutions integrable and square-integrable.

The non-square integrability associated with the first and second kinds of singularity forbids the existence of eigenvalues and eigenmodes. However, real fluids are viscous and do have (damped) eigenmodes. We therefore face the unusual situation where eigenmodes of a fluid require the viscosity to exist and be computed. As shown in Rieutord *et al.* (2001), viscosity regularizes the singularities into thin shear layers whose width scales with the one-fourth power of viscosity. Hence, it turns out that attractors which control the dynamics of characteristics also control shear layers associated with the viscous modes. It was shown in particular that the asymptotic (for low viscosities) eigenmodes result from a balance between the diffusive action of viscosity and the focusing exerted by attractors.

However, the question of how viscosity determines the eigenvalues (eigenfrequencies and damping rates) remained unsolved. Solving this problem is of considerable interest as it opens up the asymptotic theory to a large class of problems which include gravity modes and gravito-inertial modes which suffer from the same mathematical constrains. But the challenge is difficult since one needs to combine the effects of a mapping which makes the solution singular and the effects of the viscosity which regularizes and quantizes the solution. To our knowledge such a problem has never been considered.

In this paper we present a step towards the solution of this problem. As in Rieutord *et al.* (2001, hereafter referred to as I), we consider the case of a fluid inside a rotating spherical shell because of its numerous applications to astrophysical and geophysical situations. As outlined above, many difficulties need to be overcome and to make progress simplifications are in order. We found that reducing the problem to two dimensions offers an interesting step towards the general solution. Such a simplification is equivalent to considering the inertial modes inside a toroidal shell in the limit of an infinite major radius, i.e. a slender toroidal shell. It has the merit of removing the weakest singularities which are not essential to our problem (critical latitudes and axial symmetry as described above). It thus simplifies the action of the mapping (the inviscid evolution along characteristics is reduced to the identity) but the questions of how singularities are regularized and how quantization arises are still present.

As we shall see, this two-dimensional problem can be solved entirely and offers a nice physical picture: modes featured by attractors can be viewed as a (inertial) wave trapped in a potential well, like a quantum particle. We give an analytical formula

for the frequency (and damping rate) of the modes in the asymptotic limit where the Ekman number vanishes.

Besides their pedagogical virtue which permits the understanding of the regularization and quantization processes, these two-dimensional solutions also have applications to the real world as a zeroth order of a perturbative approach to three-dimensional solutions. As shown by Stewartson (1971, 1972*a*, *b*) during the first attempts to solve this problem, the equatorial region of a thin spherical shell can be dealt with as a two-dimensional approximation. This is of course of great interest for the ocean and atmosphere dynamics (Maas 2001). We give an example of a particular application.

We have organized the paper as follows: in the first part we formulate the two-dimensional problem and give the associated numerical solutions. The second part of the paper is devoted to the analysis of the solutions which is divided into two steps: the boundary layer analysis and the role of the mapping; putting the results together leads to the quantization of eigenvalues. We then show how these results can be applied to the thin shell limit. Finally, a discussion of the results concludes the paper.

## 2. Numerical solutions

### 2.1. *Equations of motion*

In paper I we considered an incompressible viscous fluid with kinematic viscosity $\nu$, contained in a spherical shell whose outer radius is $R$ and inner radius $\eta R$ with $\eta < 1$. The fluid is rotating around the $z$-axis with the angular velocity $\Omega$. Using $(2\Omega)^{-1}$ as the time scale and $R$ as the length scale, small-amplitude perturbations obey the linear equation

$$\left.\begin{aligned} &\frac{\partial \boldsymbol{u}}{\partial t} + \boldsymbol{e}_z \times \boldsymbol{u} = -\nabla p + E\Delta \boldsymbol{u}, \\ &\nabla \cdot \boldsymbol{u} = 0, \end{aligned}\right\} \tag{2.1}$$

where $\boldsymbol{u}$ is the velocity field of the perturbations and $p$ is the reduced pressure perturbation.

Imposing an axisymmetric motion and using cylindrical coordinates $(r, \varphi, z)$, we can write the velocity components as

$$u_r = -\frac{1}{r}\frac{\partial \chi}{\partial z}, \quad u_\varphi = u(r, z), \quad u_z = \frac{1}{r}\frac{\partial \chi}{\partial r},$$

where $\chi$ is the meridional stream function. We note that $\boldsymbol{u} = \nabla \times \chi \boldsymbol{e}_\phi / r + u(r, z)\boldsymbol{e}_\phi$. The equation of momentum and its curl yield the following equations for $\psi = \chi / r$ and $u$:

$$\left.\begin{aligned} &\lambda \Delta \psi + \partial_z u = E\Delta\Delta\psi, \\ &\lambda u - \partial_z \psi = E\Delta u. \end{aligned}\right\} \tag{2.2}$$

In order to obtain a strictly two-dimensional problem, we neglect all curvature terms like $1/r\partial/\partial r$, $1/r^2$, etc., and the Laplacian becomes $\Delta = \partial^2/\partial r^2 + \partial^2/\partial z^2$; this simplification is equivalent to identifying the meridional section of the spherical shell with that of a toroidal shell whose principal radius is set to infinity. On doing this, the associated inviscid problem is simply

$$\left(\frac{\partial^2}{\partial r^2} - \frac{\alpha^2}{\omega^2}\frac{\partial^2}{\partial z^2}\right)\begin{pmatrix} \psi \\ u \end{pmatrix} = 0,$$

where we set $\lambda = \mathrm{i}\omega$ and $\alpha^2 = 1-\omega^2$. The solutions of these equations are like those of the one-dimensional wave equation and we shall use them below in the mathematical analysis (§ 3). For the time being we concentrate on the formulation of the viscous problem adapted for numerical resolution.

Equations (2.2) are purely two-dimensional and we use polar coordinates to solve them; we set

$$r = \rho\cos\theta, \quad z = \rho\sin\theta;$$

thus

$$\frac{\partial}{\partial z} = \sin\theta\frac{\partial}{\partial\rho} + \frac{\cos\theta}{\rho}\frac{\partial}{\partial\theta}, \quad \Delta = \frac{\partial^2}{\partial\rho^2} + \frac{1}{\rho}\frac{\partial}{\partial\rho} + \frac{1}{\rho^2}\frac{\partial^2}{\partial\theta^2}.$$

Expanding $u$ and $\psi$ in Fourier series, namely

$$\psi = \sum_n \psi_n(\rho)\mathrm{e}^{\mathrm{i}n\theta}, \quad u = -\mathrm{i}\sum_n V_n(\rho)\mathrm{e}^{\mathrm{i}n\theta},$$

we obtain the set of equations

$$\left.\begin{aligned} \lambda V_n &= \frac{\psi'_{n-1} - \psi'_{n+1}}{2} - \frac{(n-1)\psi_{n-1} + (n+1)\psi_{n+1}}{2\rho} + E\Delta_n V_n, \\ \lambda\Delta_n\psi_n &= \frac{V'_{n-1} - V'_{n+1}}{2} - \frac{(n-1)V_{n-1} + (n+1)V_{n+1}}{2\rho} + E\Delta_n\Delta_n\psi_n, \end{aligned}\right\} \tag{2.3}$$

where we set

$$\Delta_n = \frac{\partial^2}{\partial\rho^2} + \frac{1}{\rho}\frac{\partial}{\partial\rho} - \frac{n^2}{\rho^2},$$

$$\Delta_n\Delta_n = \frac{\partial^4}{\partial\rho^4} + \frac{2}{\rho}\frac{\partial^3}{\partial\rho^3} - \frac{2n^2+1}{\rho^2}\frac{\partial^2}{\partial\rho^2} + \frac{2n^2+1}{\rho^3}\frac{\partial}{\partial\rho} + \frac{n^4-4n^2}{\rho^4}.$$

We note that the velocity components in the plane (formerly $u_r$, $u_z$) are now

$$u_\rho = \frac{1}{\rho}\frac{\partial\psi}{\partial\theta}, \quad u_\theta = -\frac{\partial\psi}{\partial\rho}. \tag{2.4}$$

Boundary conditions on the two circles ($\rho = \eta$ and $\rho = 1$) are either no-slip:

$$\psi_n = \frac{\partial\psi_n}{\partial\rho} = V_n = 0, \tag{2.5}$$

or stress-free:

$$\psi_n = \frac{\partial V_n}{\partial\rho} = \frac{\partial^2\psi_n}{\partial\rho^2} - \frac{1}{\rho}\frac{\partial\psi_n}{\partial\rho} = 0. \tag{2.6}$$

Equations (2.3) with boundary conditions (2.5) or (2.6) are discretized in the radial coordinate using Chebyshev polynomials. We finally obtain a generalized eigenvalue problem which we solve with the same techniques as those used in Rieutord & Valdettaro (1997).

### 2.2. *Results of numerical solutions*

As expected, two-dimensional eigenmodes are very similar to their three-dimensional counterpart shown in Rieutord & Valdettaro (1997) and I: the mode is concentrated along the attractor of characteristics existing at the given frequency. The main difference with three-dimensional modes is the absence of the axial singularity which

| $\tau = \mathrm{Re}\,(\lambda)$ | $\delta\omega = \mathrm{Im}\,(\lambda) - \omega_0$ | $\tau_1$ | $\omega_1$ | $n$ | $\dfrac{\tau_1}{1.04(n+1/2)}$ | $\dfrac{\omega_1}{1.04(n+1/2)}$ |
|---|---|---|---|---|---|---|
| $-1.6436 \times 10^{-5}$ | $1.6426 \times 10^{-5}$ | $-0.5197$ | 0.5194 | 0 | $-0.9995$ | 0.9989 |
| $-4.9352 \times 10^{-5}$ | $4.9277 \times 10^{-5}$ | $-1.5606$ | 1.5583 | 1 | $-1.0004$ | 0.9989 |
| $-8.2333 \times 10^{-5}$ | $8.2127 \times 10^{-5}$ | $-2.6036$ | 2.5971 | 2 | $-1.0014$ | 0.9989 |
| $-1.1538 \times 10^{-4}$ | $1.1498 \times 10^{-4}$ | $-3.6486$ | 3.6359 | 3 | $-1.0024$ | 0.9989 |
| $-1.4849 \times 10^{-4}$ | $1.4783 \times 10^{-4}$ | $-4.6957$ | 4.6747 | 4 | $-1.0033$ | 0.9989 |
| $-1.8167 \times 10^{-4}$ | $1.8068 \times 10^{-4}$ | $-5.7448$ | 5.7135 | 5 | $-1.0043$ | 0.9989 |

TABLE 1. Eigenvalues at $\eta = 0.35$ and $E = 10^{-9}$ near the attractor $\omega_0 = \sqrt{(3+\sqrt{5-4\eta})/8} \simeq 0.7824$; $\tau_1 = E^{-1/2}\tau$ and $\omega_1 = E^{-1/2}\delta\omega$. Stress-free boundary conditions have been used.

| $\tau$ | $\delta\omega$ | $\tau_1$ | $\omega_1$ | $n$ | $\dfrac{\tau_1}{3.16(n+1/2)}$ | $\dfrac{\omega_1}{3.16(n+1/2)}$ |
|---|---|---|---|---|---|---|
| $-5.0310 \times 10^{-5}$ | $-4.9456 \times 10^{-5}$ | $-1.5909$ | $-1.5639$ | 0 | $-1.0069$ | $-0.9898$ |
| $-1.5168 \times 10^{-4}$ | $-1.4828 \times 10^{-4}$ | $-4.7967$ | $-4.6889$ | 1 | $-1.0120$ | $-0.9892$ |
| $-2.5551 \times 10^{-4}$ | $-2.4682 \times 10^{-4}$ | $-8.0799$ | $-7.8050$ | 2 | $-1.0228$ | $-0.9880$ |

TABLE 2. Same as in table 1 but for modes associated with the attractor at $\omega_0 = \sqrt{3+\eta}/2 \simeq 0.9152$.

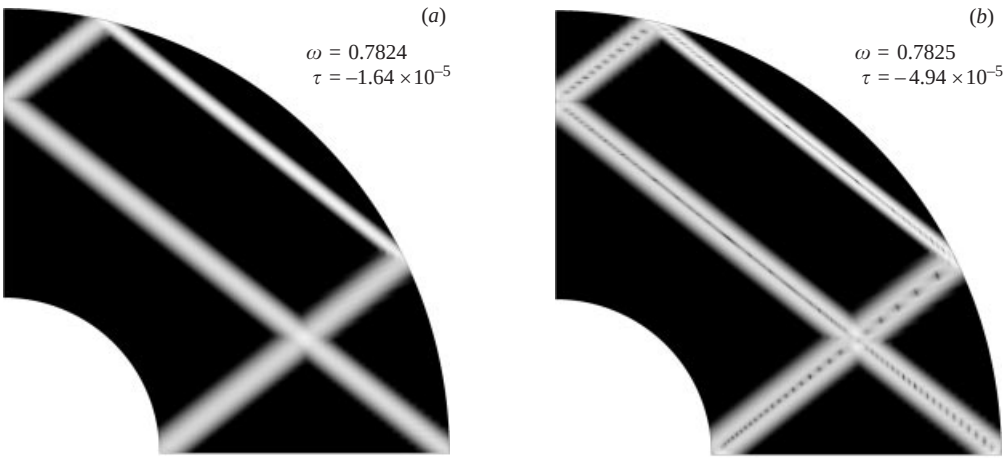


FIGURE 1. Plot of the kinetic energy in a meridional section of the spherical shell of the first two modes associated with the attractor of frequency $\omega_0 = 0.7824$; $\eta = 0.35$, $N = 1100$, $N_r = 350$, $E = 1.0 \times 10^{-9}$; see also table 1.

makes the mode amplitude almost constant along the characteristics of the attractor (see figure 1). We also observe that there is no residual amplitude outside the attractor, unlike the three-dimensional case where some 'noise' was always present; in some way, two-dimensional solutions are neater.

However, the most interesting result shown by numerical solutions is the quantization of eigenvalues of modes pertaining to a given attractor. This quantization is clearly shown by tables 1 and 2. This quantization of eigenvalues is associated with an increasing number of nodes of eigenfunctions when cut along a line perpendicular to the attractor (figure 2). Figure 3 clearly illustrates this behaviour of eigenmodes, which is similar to the solutions of a Sturm–Liouville problem.

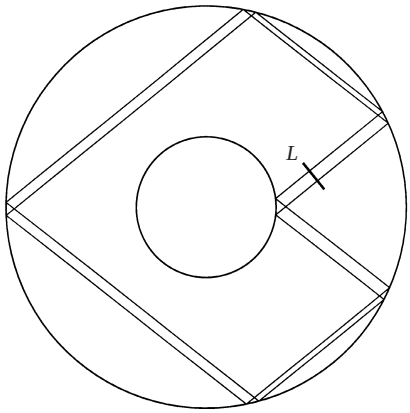


FIGURE 2. Attractors for modes of table 1 and figure 1. The straight line $L$ crossing the attractors is the one for which we have computed the profiles of figures 3 and 4.

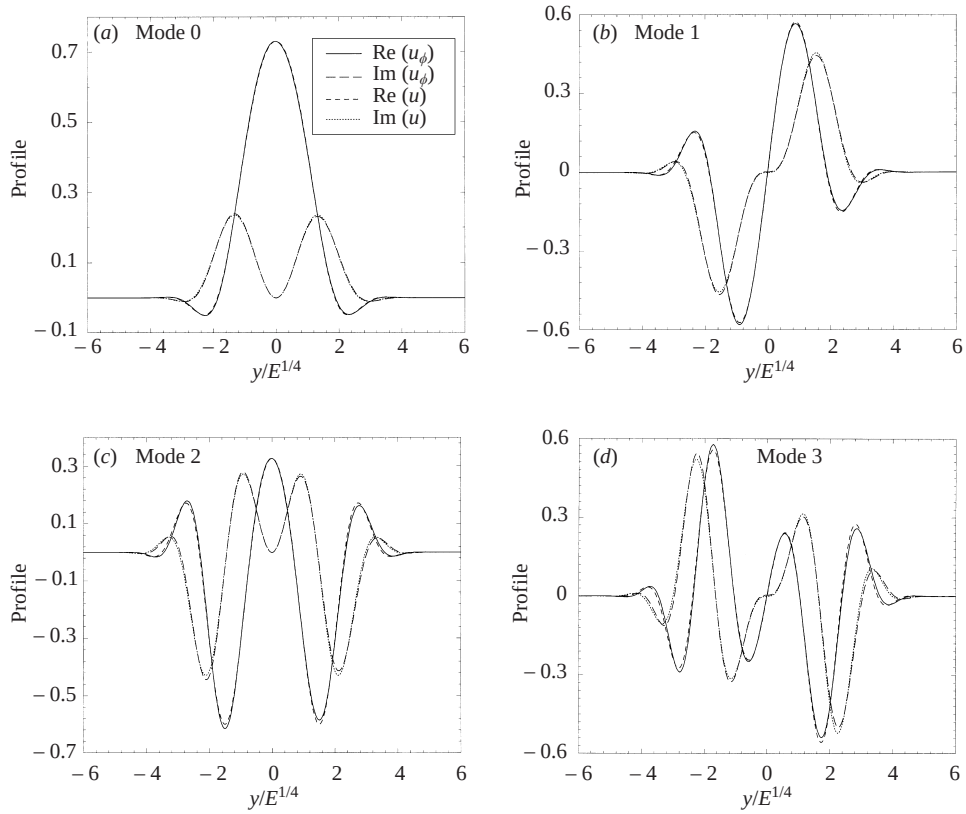


FIGURE 3. ($a$) Profile of $u_\phi$ across the straight line $L$ of figure 2 for mode $n = 0$ of table 1. We also plot the analytical solution $u$ given by (3.22). The difference between the numerical solution ($u_\phi$) and the analytical one ($u$) is hardly perceptible. ($b$–$d$) As ($a$) but for modes $n = 1$, $n = 2$ and $n = 3$ of table 1.

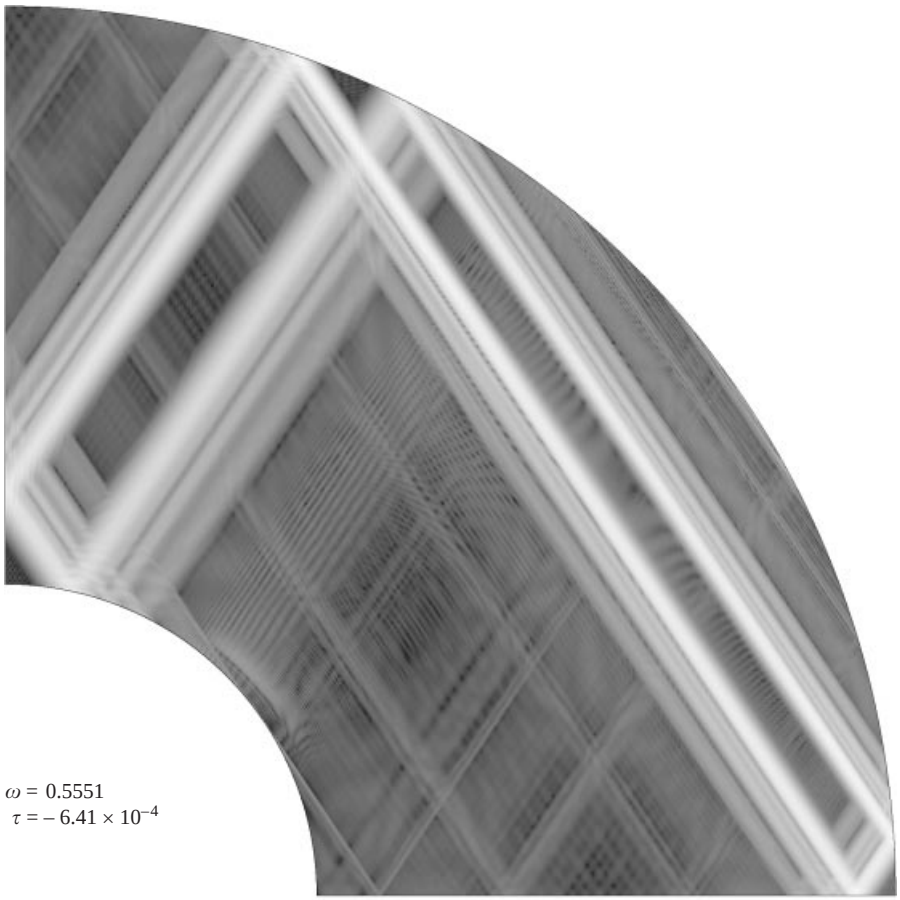


FIGURE 4. Plot of the kinetic energy in a meridional section of the spherical shell of the least-damped mode associated with the asymptotic attractor of frequency $\omega_0 = 0.55536929$; $\eta = 0.35$, $N = 1100$, $N_r = 350$, $E = 1.0 \times 10^{-9}$.

### 2.3. *Selection of attractors*

Not all attractors, however, give birth to the 'simple' solutions described above; indeed, attractors which are symmetric with respect to the origin, i.e. in the transform $\theta \rightarrow \theta + \pi$, do not have such solutions. This is a consequence of the form of equations (2.3) from which it turns out that either $\psi$ or $u$ is antisymmetric with respect to the origin. An example of this situation is given by the attractor mentioned in Rieutord *et al.* (2000): although clearly existing in three dimensions this attractor seems to be avoided in two dimensions; indeed, figure 4 shows that, although the amplitude of the mode is dominated by the attractor, the shear layers are much more spread out than those of the modes in figure 1. Attractors which are not symmetric within the transform $\theta \rightarrow \theta + \pi$ (like that of figure 1) do not suffer such constraints since they can be symmetrized (or antisymmetrized) appropriately.

We therefore see that the simple rules shown by table 1 or 2 do not apply to all attractors. However, this selection effect is specific to the two-dimensional problem which is obviously not able to mimic the three-dimensional problem in all cases.

## 3. The analytical solution

The foregoing numerical results can be completely explained by making a local analysis of the shear layers combined with the role of the mapping made by the attractor.

### 3.1. *Boundary layer analysis for the shear layers*

The boundary layer analysis was presented in I and we just need, here, to start from equation (3.6) of I, letting $s \to \infty$; thus we find that

$$\left.\begin{aligned} &\lambda u_x - \omega u_\varphi = -\frac{\partial p}{\partial x} + E\nabla^2 u_x, \\ &\lambda u_\varphi + \omega u_x - \alpha u_y = E\nabla^2 u_\varphi, \\ &\lambda u_y + \alpha u_\varphi = -\frac{\partial p}{\partial y} + E\nabla^2 u_y, \\ &\frac{\partial u_x}{\partial x} + \frac{\partial u_y}{\partial y} = 0, \end{aligned}\right\} \tag{3.1}$$

where $\nabla^2 = \partial^2/\partial x^2 + \partial^2/\partial y^2$ and $\alpha = \sqrt{1-\omega^2}$; $x$ and $y$ are respectively the coordinates along and perpendicular to the characteristic in the meridional plane.

As shown by tables 1 and 2, eigenvalues can be written

$$\lambda = \mathrm{i}\omega_0 + E^{1/2}(\tau_1 + \mathrm{i}\omega_1) + O(E)$$

where $\omega_0$ is the frequency of the asymptotic attractor, i.e. the attractor for which the Lyapunov exponent vanishes (see I).

Let us now assume that the shear layers have a typical width $E^{1/4}$ in the $y$-direction. We thus rescale $y$ to $\hat{y} = E^{-1/4}y$ and we assume in the following that $\partial/\partial\hat{y} \sim 1$. Equations (3.1) become

$$\mathrm{i}\omega u_x - \omega u_\phi = -\frac{\partial p}{\partial x} + E^{1/2}\left(\frac{\partial^2}{\partial \hat{y}^2} - \tau_1\right) u_x,$$

$$\mathrm{i}\omega u_\phi + \omega u_x - \alpha u_y = E^{1/2}\left(\frac{\partial^2}{\partial \hat{y}^2} - \tau_1\right) u_\phi,$$

$$\mathrm{i}\omega u_y + \alpha u_\phi = -E^{-1/4}\frac{\partial p}{\partial \hat{y}} + E^{1/2}\left(\frac{\partial^2}{\partial \hat{y}^2} - \tau_1\right) u_y, \tag{3.2}$$

$$\frac{\partial u_x}{\partial x} + E^{-1/4}\frac{\partial u_y}{\partial \hat{y}} = 0, \tag{3.3}$$

where we set $\omega = \omega_0 + E^{1/2}\omega_1$ and $\alpha = \alpha_0 - E^{1/2}\omega_0\omega_1/\alpha_0$.

From (3.2) the pressure must scale like $E^{1/4}$. Therefore we set $p = E^{1/4}\hat{p}$. From (3.3) we see that $u_y$ is small. We set $u_y = E^\gamma \hat{u}_y$ with $\gamma \geqslant 1/4$. We thus obtain

$$\mathrm{i}\omega u_x - \omega u_\phi = -E^{1/4}\frac{\partial \hat{p}}{\partial x} + E^{1/2}\left(\frac{\partial^2}{\partial \hat{y}^2} - \tau_1\right) u_x, \tag{3.4}$$

$$\mathrm{i}\omega u_x - \omega u_\phi = \mathrm{i}\alpha E^\gamma \hat{u}_y + \mathrm{i}E^{1/2}\left(\frac{\partial^2}{\partial \hat{y}^2} - \tau_1\right) u_\phi, \tag{3.5}$$

$$\alpha u_\phi + \frac{\partial \hat{p}}{\partial \hat{y}} = \left[-\mathrm{i}\omega + E^{1/2}\left(\frac{\partial^2}{\partial \hat{y}^2} - \tau_1\right)\right] E^\gamma \hat{u}_y,$$

$$\frac{\partial u_x}{\partial x} + E^{\gamma - 1/4}\frac{\partial \hat{u}_y}{\partial \hat{y}} = 0.$$

To leading order we obtain

$$u_x = -\mathrm{i}u_\phi, \tag{3.6}$$

$$u_\phi = -\frac{1}{\alpha_0}\frac{\partial \hat{p}}{\partial \hat{y}}, \tag{3.7}$$

$$\frac{\partial u_x}{\partial x} + E^{\gamma-1/4}\frac{\partial \hat{u}_y}{\partial \hat{y}} = 0, \tag{3.8}$$

and to next order (3.5) and (3.4) give

$$\mathrm{i}\alpha_0 E^\gamma \hat{u}_y + E^{1/4}\frac{\partial \hat{p}}{\partial x} + \mathrm{i}E^{1/2}\left(\frac{\partial^2}{\partial \hat{y}^2} - \tau_1\right)u_\phi - E^{1/2}\left(\frac{\partial^2}{\partial \hat{y}^2} - \tau_1\right)u_x = 0. \tag{3.9}$$

From (3.8) we see that $\partial/\partial x \sim E^{\gamma-1/4}$. Substituting in (3.9) shows that the only value of $\gamma$ for which the inertial terms balance the viscous ones is $\gamma = 1/2$. We shall therefore set in the following $\gamma = 1/2$ and $\hat{x} = E^{1/4}x$. Let us stress that the very weak variation along the characteristics is necessary for the existence of $\frac{1}{4}$-layers. Unlike standard boundary layers, $\frac{1}{4}$-layers terms following leading order $O(1)$ terms are of second order, namely $O(E^{1/2})$.

For simplicity we shall drop from now on the hats from all the variables. From (3.6) and (3.7) we obtain $u_x = \mathrm{i}\alpha_0^{-1}\partial p/\partial y$. Substituting in (3.8) we obtain

$$\frac{\partial}{\partial y}\left(u_y + \frac{\mathrm{i}}{\alpha_0}\frac{\partial p}{\partial x}\right) = 0. \tag{3.10}$$

We now derive (3.9) with respect to $y$ and we use (3.6), (3.7) and (3.10) to write $u_x$, $u_y$ and $u_\phi$ in terms of pressure:

$$\frac{\partial}{\partial y}\left(\frac{\partial^3 p}{\partial y^3} - \tau_1\frac{\partial p}{\partial y} + \mathrm{i}\alpha_0\frac{\partial p}{\partial x}\right) = 0. \tag{3.11}$$

Recalling (3.6) and (3.7) we see that the velocity components $u_x$ and $u_\phi$ obey the same equation:

$$\frac{\partial^3 u}{\partial y^3} - \tau_1\frac{\partial u}{\partial y} + \mathrm{i}\alpha_0\frac{\partial u}{\partial x} = 0. \tag{3.12}$$

To summarize, the proper scalings are

$$u_x \sim u_\phi \sim 1, \quad p \sim \frac{\partial}{\partial x} \sim E^{1/4}, \quad u_y \sim E^{1/2}, \quad \frac{\partial}{\partial y} \sim E^{-1/4}.$$

Note that if this is introduced from the beginning into the equation for the pressure, namely into

$$E^2\Delta^3 p - 2E\lambda\Delta^2 p + \lambda^2\Delta p + \frac{\partial^2 p}{\partial z^2} = 0, \tag{3.13}$$

(3.11) is obtained very easily.

### 3.2. *The part played by the mapping*

Equation (3.11) must be satisfied by the shear layer solutions of the eigenvalue problem, yet it is not sufficient to describe completely their structure. What is lacking

is that we have to take into account the boundary conditions and the fact that the orbit spanned by the shear layers is closed.

In particular, in order to satisfy the full eigenvalue problem we must impose that a shear layer with a given profile $f(y) = u(x_0, y)$ at a given $x_0$ will be mapped exactly onto itself after propagating along the characteristics that constitute the periodic mapping. Thus, one needs to incorporate the global effects of the mapping coming from the reflection properties of the characteristics with the local character of a boundary layer analysis. As we shall see, this can be done analytically in the two-dimensional problem.

First, we observe that in terms of the rescaled variable $x$, the size of the container is $O(E^{1/4})$, thus very small. Hence, if we consider the $n$th branch, of length $\ell_n$, of the shear layer, we can express the variation of the solution along this branch as

$$u_n(x_n + \ell_n, y) \simeq u_n(x_n, y) + \left.\frac{\partial u_n(x, y)}{\partial x}\right|_{x_n} \ell_n E^{1/4},$$

where $u_n$ is one component of the velocity field and $x_n$ the abscissa at the beginning of the branch. In the following, $u$ will represent either $u_\phi$ or $u_x$; it satisfies (3.12), therefore

$$\frac{\partial u_n}{\partial x} = \frac{\mathrm{i}}{\alpha_0}\left(\frac{\partial^3 u_n}{\partial y^3} - \tau_1 \frac{\partial u_n}{\partial y}\right),$$

which gives the evolution of the velocity field due to viscosity along the $n$th branch.

We first consider stress-free boundary conditions. In this case a shear layer reflecting on a boundary will only be rescaled by a geometrical factor depending on the inclination of the tangent to the boundary. A solution at the beginning of branch $n$ ($u_n$) is, to order $E^0$, just a rescaled version of the solution of any other branch, namely

$$u_n(x_n, y) = \frac{1}{K_n} u\left(x_1, \frac{y}{K_n}\right),$$

where $K_n$ is a product of contraction/dilation coefficients arising from the reflections on the boundaries (the $C_n$ in Appendix B of I). Thus on branch $n$ we obtain

$$\delta u_n \equiv u_n(x_n + \ell_n, y) - u_n(x_n, y) = \frac{\mathrm{i}\ell_n E^{1/4}}{\alpha_0 K_n}\left[\frac{1}{K_n^3}\frac{\partial^3 u(x_1, y/K_n)}{\partial (y/K_n)^3} - \frac{\tau_1}{K_n}\frac{\partial u(x_1, y/K_n)}{\partial (y/K_n)}\right].$$

The perturbations $\delta u_n$ propagate along the characteristics and are rescaled upon reflection on the boundaries; when they reach the first branch the velocity variation is rescaled by the factor $K_n$, so that

$$\delta u_n = \left[\frac{1}{K_n^3}\frac{\partial^3 u(x_1, y)}{\partial y^3} - \frac{\tau_1}{K_n}\frac{\partial u(x_1, y)}{\partial y}\right]\frac{\mathrm{i}\ell_n}{\alpha_0} E^{1/4}. \tag{3.14}$$

The total perturbation of the initial profile after one complete loop along the periodic attractor is the sum of the contributions (3.14) of all the branches:

$$\delta u = \sum_n \delta u_n = \frac{\partial}{\partial y}\left[\frac{\mathrm{i}A}{\alpha_0}\frac{\partial^2 u}{\partial y^2} - \frac{\mathrm{i}\tau_1 B}{\alpha_0} u\right] E^{1/4}, \tag{3.15}$$

where we have defined $A$ and $B$ as

$$A = \sum_{n=1}^{N} \frac{\ell_n}{K_n^3}, \quad B = \sum_{n=1}^{N} \frac{\ell_n}{K_n}.$$

Equation (3.15) gives the variation of the velocity due to viscosity along the path of characteristics of the periodic orbit; it does not include the variations due to the mapping, namely the fact that the point $(x_0, y)$ will be shifted to a different point $(x_0, y')$ after one iteration of the mapping when returning on the same branch after one loop.

In order to evaluate this variation we shall use the mapping $f(\phi, \lambda^c)$ expressed in terms of the latitude $\phi$ and the critical latitude $\lambda^c$ (which is equivalent to the frequency of the mode). We use the same definition as in I, namely

$$f : [0, 4\pi] \longrightarrow [0, 4\pi],$$

$$\phi \longrightarrow \phi' = f(\phi, \lambda^c), \tag{3.16}$$

where $\phi'$ is the latitude of the reflection point of the characteristic after one loop in the neighbourhood of an attractor†; if $\phi$ references a point of the attractor then $\phi' = \phi$. A simple example of a mapping is given by the equatorial attractor described in I (§ B.1.1); the mapping for which $\phi_3$ is a fixed point is

$$f(\phi, \lambda^c) = \arccos\left[\cos(\phi - \lambda^c)\cos 2\lambda^c + \sin 2\lambda^c \sqrt{\eta^2 - \cos^2(\phi - \lambda^c)}\right] - 5\lambda^c.$$

Now, let us denote as $\lambda_0^c$ the critical latitude at which the Lyapunov exponent is zero, and $\phi_0$ the fixed point for the mapping at $\lambda_0^c$ (that is $f(\phi_0, \lambda_0^c) = \phi_0$). The relation between the coordinate $y$ perpendicular to the characteristic and the latitude $\phi$ is, for $\phi$ very near $\phi_0$, $y = pE^{-1/4}(\phi - \phi_0)$, with $p = r\sin(\phi_0 \pm \lambda_0^c)$, $r(= \eta$ or $1)$ being the radius of the starting point of the first branch, and $\pm$ the sign of the slope of the characteristic of the shear layer in the first branch. We define the rescaled critical latitude $\hat{\lambda} = E^{-1/2}(\lambda^c - \lambda_0^c)$. We shall assume in the following that $y$ and $\hat{\lambda}$ are $O(1)$. Denoting as $\hat{f}(y, \hat{\lambda})$ the mapping expressed in terms of the rescaled variables, we have the following relations:

$$\hat{f}(y, \hat{\lambda}) = pE^{-1/4}(f(\phi, \lambda^c) - f(\phi_0, \lambda_0^c)),$$

$$\frac{\partial^{i+j}\hat{f}}{\partial y^i \partial \hat{\lambda}^j} = (pE^{-1/4})^{1-i} E^{j/2} \frac{\partial^{i+j} f}{\partial \phi^i \partial \lambda^{cj}}.$$

We shall use the notation

$$f_{ij} \equiv \left.\frac{\partial^{i+j} f}{\partial \phi^i \partial \lambda^{cj}}\right|_{\phi_0, \lambda_0^c}, \quad \hat{f}_{ij} \equiv \left.\frac{\partial^{i+j}\hat{f}}{\partial y^i \partial \hat{\lambda}^j}\right|_{0,0} = (pE^{-1/4})^{1-i} E^{j/2} f_{ij}.$$

The contraction due to the mapping is given by

$$u_N(\hat{f}(y, \hat{\lambda}))\, \mathrm{d}\hat{f} = u(y, \hat{\lambda})\, \mathrm{d}y; \tag{3.17}$$

$u_N$ is the velocity that would be obtained after one loop ($N$ is the number of branches) by transporting the initial profile $u$ along the path of characteristics subject to the inviscid hyperbolic equations. This relation expresses the fact that the flux of the mapped velocity does not vary.

We develop (3.17) in Taylor series around $y = 0$, $\hat{\lambda} = 0$ and retain terms up to $E^{1/4}$.

† Although the definition of $f$ is general, that of a loop makes sense only in the neighbourhood of an attractor.

We recall from Appendix B of I that $f_{10} = 1$ and $\hat{f}(0,0) = 0$. Thus we have

$$\hat{f}(y,\hat{\lambda}) = \hat{f}(0,0) + \hat{f}_{10}y + \hat{f}_{01}\hat{\lambda} + \tfrac{1}{2}\hat{f}_{20}y^2 + \cdots$$

$$= y + pf_{01}\hat{\lambda}E^{1/4} + \frac{f_{20}}{2p}y^2E^{1/4} + \cdots,$$

$$\frac{\partial \hat{f}(y,\hat{\lambda})}{\partial y} = \hat{f}_{10} + \hat{f}_{20}y + \cdots = 1 + \frac{f_{20}}{p}yE^{1/4} + \cdots.$$

Defining

$$\delta \equiv pf_{01}\hat{\lambda} + \tfrac{1}{2}f_{20}y^2$$

we see that (3.17) becomes

$$u(y) \simeq u_N(y + \delta E^{1/4}) \left.\frac{\partial \hat{f}}{\partial y}\right|_{y,\hat{\lambda}};$$

therefore, neglecting deviations of order $E^{1/2}$:

$$u_N(y) \simeq \frac{u(y-\delta E^{1/4})}{\partial \hat{f}/\partial y|_{y-\delta E^{1/4},\hat{\lambda}}} \simeq \frac{u(y-\delta E^{1/4})}{\partial \hat{f}/\partial y|_{y,\hat{\lambda}}}$$

$$\simeq \left(1 - \frac{yf_{20}E^{1/4}}{p}\right)\left(u(y) - \delta\frac{\mathrm{d}u(y)}{\mathrm{d}y}E^{1/4}\right)$$

$$\simeq u - E^{1/4}\left(\frac{f_{20}}{p}yu + pf_{01}\hat{\lambda}\frac{\mathrm{d}u}{\mathrm{d}y} + \frac{f_{20}}{2p}y^2\frac{\mathrm{d}u}{\mathrm{d}y}\right)$$

$$= u - E^{1/4}\frac{\mathrm{d}}{\mathrm{d}y}\left(\frac{f_{20}}{2p}y^2u + pf_{01}\hat{\lambda}u\right). \tag{3.18}$$

From (3.15) and (3.18) we obtain the total variation $\Delta u$ of the given profile $u(y)$ after one period along one attractor. We have

$$E^{-1/4}\Delta u = \frac{\mathrm{d}}{\mathrm{d}y}\left(\frac{\mathrm{i}A}{\alpha_0}\frac{\mathrm{d}^2u}{\mathrm{d}y^2} - \frac{f_{20}}{2p}y^2u - pf_{01}\hat{\lambda}u - \frac{\mathrm{i}\tau_1 B}{\alpha_0}u\right). \tag{3.19}$$

Let us now note that $pf_{01} = \pm B$ (the demonstration is sketched out in the Appendix) and that $\omega_1 = \alpha_0\hat{\lambda}$; hence the total variation is simply

$$E^{-1/4}\Delta u = \frac{\mathrm{d}}{\mathrm{d}y}\left(\frac{\mathrm{i}A}{\alpha_0}\frac{\mathrm{d}^2u}{\mathrm{d}y^2} - \frac{f_{20}}{2p}y^2u - \frac{\mathrm{i}\lambda_1 B}{\alpha_0}u\right), \tag{3.20}$$

where we set $\lambda_1 = \tau_1 \pm \mathrm{i}\omega_1$.

### 3.3. *Quantization of eigenvalues*

The final step is to require that for the solution obtained, there is no variation of the velocity after one loop along the attractor; hence we impose $\Delta u = 0$:

$$\frac{\mathrm{i}A}{\alpha_0}\frac{\mathrm{d}^2u}{\mathrm{d}y^2} - \frac{f_{20}}{2p}y^2u - \frac{\mathrm{i}\lambda_1 B}{\alpha_0}u = 0. \tag{3.21}$$

This equation is easily solved by changing the coordinate: $z = \mathrm{e}^{-\mathrm{i}\pi/8}(pA/2\alpha_0 f_{20})^{-1/4}y$.

| $\omega_0$ | $A$ | $B$ | $\alpha_0$ | $p$ | $f_{01}$ | $f_{20}$ | $2\omega_1$ $(n=0)$ | $2\omega_1$ (num) |
|---|---|---|---|---|---|---|---|---|
| 0.403 | 22.5386 | 5.4017 | 0.9152 | 0.9473 | 5.7021 | 29.8094 | 4.7164 | 4.708 |
| 0.623 | 27.4620 | 9.2119 | 0.7824 | 0.9760 | 9.4388 | 5.2267 | 1.1645 | 1.164 |
| 0.662 | 54.3756 | 16.9851 | 0.7491 | 0.2622 | 64.7850 | 1.6403 | 0.9399 | 0.9396 |
| 0.782 | 27.4620 | 9.2119 | 0.6228 | 0.2738 | 33.6390 | 1.4665 | 1.0389 | 1.039 |
| 0.915 | 22.5386 | 5.4017 | 0.4031 | 0.9473 | 5.7021 | 29.8094 | 3.1302 | 3.128 |

TABLE 3. Comparison between theoretical and analytical eigenvalues along with coefficients of the mapping. Only absolute values of the parameters are given.

It becomes

$$\frac{\mathrm{d}^2u}{\mathrm{d}z^2} - \left[\tfrac{1}{4}z^2 + \mathrm{e}^{\mathrm{i}\pi/4}B\left(\frac{p}{2\alpha_0 A f_{20}}\right)^{1/2}(\tau_1 \pm \mathrm{i}\omega_1)\right]u = 0.$$

This differential equation is actually the Schrödinger equation of a quantum particle trapped in a parabolic well, i.e. the famous harmonic oscillator. Its solutions are the parabolic cylinder functions:

$$u = U(a,z), \quad a = \mathrm{e}^{\mathrm{i}\pi/4}B\left(\frac{p}{2\alpha_0 A f_{20}}\right)^{1/2}(\tau_1 \pm \mathrm{i}\omega_1).$$

As $-\pi/4 < \arg(z) < \pi/4$, there exist values of $a$ for which $U(a,z)$ vanishes at both $z \to -\infty$ and $z \to +\infty$: these are $a = -n - 1/2$, with $n$ integer; for these values the solution is simply

$$u = U(-n-1/2, z) = \mathrm{e}^{-z^2/2}H_n(z), \tag{3.22}$$

where $H_n(z) = (-1)^n \mathrm{e}^{z^2}\mathrm{d}^n\mathrm{e}^{-z^2}/\mathrm{d}z^n$ are the Hermite polynomials.

The condition $a = -n - 1/2$ yields the quantization rule:

$$\tau_1 = \pm\omega_1 = -(n+\tfrac{1}{2})\sqrt{\frac{\alpha_0 A f_{20}}{pB^2}} \tag{3.23}$$

which is verified by numerical solutions as shown by table 3.

These solutions are valid for stress-free boundary conditions; however, they may easily be generalized to a container with no-slip boundary conditions. Indeed, such boundary conditions introduce Ekman layers at the reflection point of the shear layers. Standard boundary layer theory can be applied and leads to eigenvalues of the form

$$\lambda = \lambda_{SF} + (K_\tau + \mathrm{i}K_\omega)\sqrt{E}, \tag{3.24}$$

where the constants $K_\tau$ and $K_\omega$ weakly depend on the index $n$ of the mode. As an example, we give in table 4 the eigenvalues associated with the attractor of figure 1 for no-slip boundary conditions.

## 4. Application to the spherical shell

The two-dimensional solutions which have been obtained can readily be applied to the three-dimensional problem when the modes remain far from the symmetry axis. In such a case, two-dimensional solutions behave as approximations of three-dimensional axisymmetric ones since they only lack curvature terms. Such a situation occurs naturally with equatorially trapped modes in a thin spherical shell (Stewartson 1971).

| $\tau$ | $\delta\omega$ | $n$ | $K_\tau$ | $K_\omega$ |
|---|---|---|---|---|
| $-5.4270 \times 10^{-5}$ | $2.2239 \times 10^{-5}$ | 0 | $-1.20$ | 0.183 |
| $-8.7205 \times 10^{-5}$ | $5.5068 \times 10^{-5}$ | 1 | $-1.20$ | 0.181 |
| $-1.2020 \times 10^{-4}$ | $8.7895 \times 10^{-5}$ | 2 | $-1.20$ | 0.179 |
| $-1.5327 \times 10^{-4}$ | $1.2072 \times 10^{-4}$ | 3 | $-1.21$ | 0.178 |
| $-1.8640 \times 10^{-4}$ | $1.5355 \times 10^{-4}$ | 4 | $-1.21$ | 0.176 |
| $-2.1959 \times 10^{-4}$ | $1.8638 \times 10^{-4}$ | 5 | $-1.22$ | 0.174 |

TABLE 4. Same as table 1 but with no-slip boundary conditions. The constants $K_\tau$ and $K_\omega$ are defined in (3.24).

| $n$ | 3D observations | | 2D Model |
|---|---|---|---|
| | $-\tau_1/K$ | $\omega_1/K$ | $-\tau_1/K$ |
| 0 | 0.497 | 0.484 | 0.5 |
| 1 | 1.51 | 1.499 | 1.5 |
| 2 | 2.53 | 2.49 | 2.5 |
| 3 | 3.565 | 3.50 | 3.5 |
| 4 | 4.60 | 4.49 | 4.5 |
| 5 | 5.67 | 5.50 | 5.5 |
| 6 | 6.69 | 6.53 | 6.5 |
| 7 | 7.63 | 7.50 | 7.5 |

TABLE 5. Comparison between the predictions of the two-dimensional model with the numerical solutions of three-dimensional equations for equatorially trapped modes in a thin shell ($\eta = 0.95$). $K = \sqrt{\alpha_0 A f_{20}/pB^2} = 23.8709$ is the constant appearing in (3.23) of the two-dimensional model. The modes are those described in I associated with the equatorial attractor whose asymptotic frequency is $\omega_0 = \sqrt{1-\eta}/2$.

As an illustration of such a situation we computed the modes associated with the equatorial attractor at $\omega_0 = \sqrt{1-\eta}/2$ (cf. I figure 7*a*) for a thin shell with $\eta = 0.95$. As shown by table 5, the agreement between the predictions of the two-dimensional model and the values computed from the numerical solutions of the three-dimensional problem is quite good, especially for the frequency shift $\omega_1$. This example shows that the two-dimensional model can be safely used for geophysical applications dealing with equatorially trapped modes in the atmosphere or the ocean for which $1 - \eta \approx 10^{-3}$. Furthermore, as a test of robustness, we made the same comparison but for a thick shell with $\eta = 0.35$ (like the liquid core of the Earth) still using the equatorial attractor; quite surprisingly, the predicted eigenvalues are not far from the observed ones; for instance, the $n = 1$ mode is predicted with $\tau_1 = -7.07$ and observed at $\tau_1 = -6.75$, $\omega_1 = 6.66$.

These results show an interesting property of the two-dimensional solutions: they can be used as the zeroth-order solutions in a perturbative approach to the three-dimensional solutions. One can indeed include perturbatively, as long as the modes do not touch the axis of symmetry, the curvature terms so as to obtain a better approximation of the three-dimensional solution.

## 5. Discussion

We have shown that the eigenvalue problem of inertial modes in a toroidal shell in the limit of large principal radius, which is the two-dimensional analogy of the spherical shell problem, is solvable analytically for modes focused along an attractor.

The physical picture is that an inertial wave is trapped by the attractor and resists collapse because of diffusion (viscosity). The focused mode is strictly analogous to the probability wave function of a quantum particle trapped in a potential well $V(x) = x^2$. This leads to a simple quantization of eigenvalues where the profile of the modes is given by parabolic cylinder functions. Shear layers are simple $E^{1/4}$-layers with no inner $E^{1/3}$-layer as in steady Stewartson layers.

Contemplating these results one wonders how they may generalize in three dimensions. The case of the inertial modes in a spherical shell bears some resemblance to the two-dimensional case studied here: the attractors in a meridional plane have the same shape, the numerical solutions in both cases display $E^{1/4}$ shear layers focused along an attractor and the eigenvalues depart from the asymptotic value by a shift of order $E^{1/2}$. Hence, the general idea of separating the effects of the local balance of forces, implied by the equations of motions, and the global effect of the mapping can also be applied. But these two steps are both more complicated. In I, we noticed that shear layers may in fact be nested layers combining the $E^{1/3}$- and $E^{1/4}$-scales as Stewartson layers; however, the way the $E^{1/4}$-scale is determined is still an open question. Then, the evolution imposed by the mapping along a characteristic path towards an attractor is governed by Riemann integrals (see I). Finally, the eigenvalues which are computed numerically for modes associated with attractors touching the symmetry axis do not show simple rules of quantization, implying an involved quantization process.

Nevertheless, the two-dimensional results are of practical interest: they may be used for a very thin spherical shell as shown in early approaches to this problem (see Stewartson 1972*b*); we have shown that in this case, the two-dimensional analytical predictions are very close to the three-dimensional solutions (obtained numerically); hence, the two-dimensional solutions are the first step of a perturbative approach towards the more complex three-dimensional one as long as the axis is not touched. Moreover, it is clear that our method is easily applicable to other two-dimensional problems when the geometry is different from that of the spherical shell. The relevant coefficients ($A$, $B$, $f_{20}$, $f_{01}$, $p$) just need to be computed for the new container and the desired attractor. Thus inertial modes like those studied by Maas (2001), where the third dimension does not seem to play an important part, can certainly be approached with our method.

The numerical calculations have been carried out on the NEC SX5 of the 'Institut du Développement et des Ressources en Informatique Scientifique' (IDRIS) which is gratefully acknowledged.

## Appendix. The relation $pf_{01} = \pm B$

We wish to compute $\partial f/\partial\lambda$ at the fixed point of the asymptotic attractor:

$$\begin{aligned}
\delta y_n &= \ell_n \delta\lambda + \frac{\partial y_n}{\partial \phi_{n-1}} \delta\phi_{n-1} \\
&= \ell_n \delta\lambda + \frac{p_n}{p_{n-1}} \frac{\partial \phi_n}{\partial \phi_{n-1}} \delta y_{n-1} \\
&= \ell_n \delta\lambda + \frac{p_n \delta\phi_n}{p_{n-1}\delta\phi_{n-1}} \delta y_{n-1} \\
&= \ell_n \delta\lambda + \frac{\delta y_{n-1}}{C_n}.
\end{aligned}$$

The last equation is a recurrence relation. Setting $\delta y_0 = 0$, we obtain

$$\delta y_n = \left( \ell_n + \frac{\ell_{n-1}}{C_n} + \frac{\ell_{n-2}}{C_n C_{n-1}} + \cdots + \frac{\ell_1}{C_n C_{n-1} \cdots C_2} \right) \delta\lambda,$$

from which we deduce that $p_n f_{01} = \pm B$ since $\delta y_n = p_n \delta\phi_n = p_n f_{01} \delta\lambda$. The $\pm$ sign comes from the choice of the mapping, namely whether we choose $f$ or $f^{-1}$.

## REFERENCES


Greenspan, H. P. 1969 *The Theory of Rotating Fluids*. Cambridge University Press.

Maas, L. 2001 Waves focusing and ensuing mean flow due to symmetry breaking in rotating fluids. *J. Fluid Mech.* **437**, 13–28.

Maas, L. & Lam, F.-P. 1995 Geometric focusing of internal waves. *J. Fluid Mech.* **300**, 1–41.

Rieutord, M., Georgeot, B. & Valdettaro, L. 2000 Waves attractors in rotating fluids: a paradigm for ill-posed cauchy problems. *Phys. Rev. Lett.* **85**, 4277–4280.

Rieutord, M., Georgeot, B. & Valdettaro, L. 2001 Inertial waves in a rotating spherical shell: attractors and asymptotic spectrum. *J. Fluid Mech.* **435**, 103–144 (referred to herein as I).

Rieutord, M. & Valdettaro, L. 1997 Inertial waves in a rotating spherical shell. *J. Fluid Mech.* **341**, 77–99.

Stewartson, K. 1971 On trapped oscillations of a rotating fluid in a thin spherical shell. *Tellus* **23**, 506–510.

Stewartson, K. 1972*a* On trapped oscillations of a rotating fluid in a thin spherical shell II. *Tellus* **24**, 283–287.

Stewartson, K. 1972*b* On trapped oscillations in a slightly viscous rotating fluid. *J. Fluid Mech.* **54**, 749–761.